Journal of the Optical Society of Korea
Vol. 17, No. 2, April 2013, pp. 182-187
DOI: http://dx.doi.org/10.3807/JOSK.2013.17.2.182

Comparative Experimental Analysis of Thermal Characteristics of Ytterbium-Doped Phosphosilicate and Aluminosilicate Fibers

Seungjong Lee[1], Luis A. Vazquez-Zuniga[1], Dongyoung Lee[1], Hyuntai Kim[1], Jayanta K. Sahu[2], and Yoonchan Jeong[1]*

[1]*Laser Engineering and Applications Laboratory, Department of Electrical and Computer Engineering, Seoul National University, Seoul 151-744, Korea*
[2]*Optoelectronics Research Centre, University of Southampton, Highfield, Southampton, SO17 1BJ, UK*

(Received March 18, 2013 : revised April 1, 2013 : accepted April 5, 2013)

We present a comparative experimental analysis of the thermal spectroscopic characteristics of a phosphosilicate (P)-based ytterbium-doped fiber (YDF) against an aluminosilicate (Al)-based YDF in the temperature range of 25 to 150ºC. We also characterize the fibers as gain media in a cladding-pumped amplifier configuration. While both fibers exhibit comparable trends in their thermal characteristics, there are noticeable distinctions in the fluorescence lifetime reduction rate and the spectral dependence of the transition cross-sections. The P- and Al-based YDFs present thermal lifetime reduction rates of 0.012%/ºC and 0.026%/ºC, respectively. In particular, in the spectral region at ~940 nm, the absorption cross-section of the P-based YDF undergoes significantly less thermal change compared to that of the Al-YDF. In the cladding-pumped amplifier configuration operating at a total gain of 10 dB, the Al-based YDF generally performs betters than the P-based YDF in the temperature range of 25 to 75ºC. However, it is highlighted that in the high temperature range of over 75ºC, the latter shows a less gain reduction rate than the former, thereby yielding higher relative output power by 3.3% for a 1060-nm signal, for example.

Keywords : Ytterbium-doped fibers, Ytterbium-doped fiber lasers, Phosphosilicate fibers, Aluminosilicate fibers
OCIS codes : (140.3510) Lasers, fiber; (140.3615) Lasers, ytterbium; (120.6810) Thermal effects; (300.6360) Spectroscopy, laser

I. INTRODUCTION

Ytterbium (Yb) has been an outstanding choice as a doping material for rare-earth-doped fibers because of its exceptional spectroscopic properties, such as simple electronic states and small quantum defect, which in fact facilitate the power extraction from the gain medium with high efficiency [1-3]. However, thermal aspects with Yb-doped fibers (YDFs) cannot be simply overlooked if they operate in high-power regimes because their thermal properties are invariably linked to their long-term reliability as well as their overall efficiency [4-11]. For example, the efficiency of an YDF as a gain medium is dependent on the spectroscopy of Yb^{3+} ions that changes with temperature [5-7], and, in particular, photo-darkening (PD) effects are significantly affected with temperature [8-11]. Consequently, thermal characteristics, together with nonlinear scattering characteristics, can eventually be limiting factors to the performance of an YDF [12-13]. Thus, they have been intensively investigated from various prospects [4-11]. However, most of the related results have been limited to aluminosilicate (Al)-based YDFs [6,7] since they have predominantly been utilized in many high-power applications [1-3]. One of the reasons must be that they present higher transition cross-sections around the 1-μm region compared to those of YDFs based on other host materials like phosphosilicate [14-16] as well as offering relatively low refractive core indices [1]. However, a main problem with Al-based YDFs is their vulnerability to PD [8-11, 16-18], particularly in fibers of high doping concentrations of Yb^{3+} ions [18]. Therefore, other types of YDFs have been considered as a replacement for Al-based YDFs

*Corresponding author: yoonchan@snu.ac.kr
Color versions of one or more of the figures in this paper are available online.

[15, 19, 20]. Among the alternatives, phosphosilicate (P)-based YDFs have received a lot of attention since they can offer a superior property to Al-based YDFs in terms of PD resilience [19, 21]. Although there were some reports limited to the general spectroscopic characteristics of P-based YDFs [14, 16], to the best of our knowledge, there has been no detailed report on their thermal characteristics as gain fibers in high-power regimes. Here, building on our previous investigations [7], we present a comprehensive, comparative experimental analysis on the thermal characteristics of a P-based YDF against an Al-based YDF, including their spectroscopic properties, Stark energy levels, and gain characteristics in a cladding-pumped amplifier configuration. Finally, we discuss all the distinctive thermal characteristics between them.

II. EXPERIMENTAL RESULT

In addition to the Al-based YDF (YDF2/Al) previously studied in Ref. 7, a P-based YDF (YDF1/P) was newly fabricated by the modified chemical-vapor deposition and solution doping technique. Its core had a diameter of 6.1 μm and a numerical aperture (NA) of 0.14. Its inner cladding was square-shaped with a side of ~130 μm and had a cladding-absorption rate of ~1.8 dB/m at 974 nm. YDF2/Al had a core diameter of 6.6 μm with an NA of 0.12. Its inner cladding was hexagon-shaped with a diagonal of ~130 μm and had a cladding absorption rate of ~2.4 dB/m at 976 nm. In both fibers the inner cladding NA was higher than 0.45. In addition, it should be noted that all the experimental measurements were done based on the methods and procedures introduced in our previous study unless stated otherwise (see Ref. 7 for details). We used a temperature-controlled oven to vary the fiber temperature from 25ºC to 150ºC. It is noteworthy that the maximum temperature was limited by the thermal damage of the outer cladding material of the fiber that was made of low-index polymer [12].

Apart from other commonly used rare-earth ions, such as erbium (Er^{3+}), neodymium (Nd^{3+}), and thulium (Tm^{3+}) ions, the energy-level structure of Yb^{3+} ions has only two manifolds, the ground state $^2F_{7/2}$ and the excited state $^2F_{5/2}$ (see Table I) [6, 7, 14]. Each state is further split into Stark sublevels: The ground state $^2F_{7/2}$ which has four sublevels (labeled from "*a*" to "*d*"), and the excited state $^2F_{5/2}$ with three sublevels (labeled from "*e*" to "*g*"). The energy of the individual sublevel varies precisely depending on the composition of the host material [14]. In fact, the energy levels of Yb^{3+} ions and the transitions among the sublevels have close relationships with the transition (absorption and emission) cross-sections as well as the fluorescence lifetime [22, 23].

In order to determine the fluorescence lifetime, a 915-nm laser diode driven in pulse mode was used to pump a short piece of YDF1/P, exciting the Yb^{3+} ions doped in the core. Fig. 1 shows the measured fluorescence lifetime

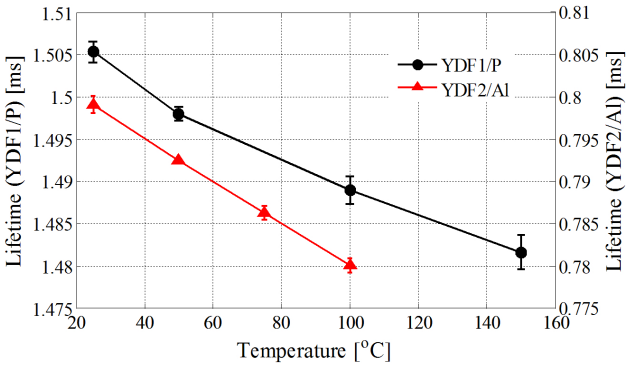

FIG. 1. Fluorescence lifetime of YDF1/P and YDF2/Al as a function of temperature. The error bars indicate the standard deviations of the measurements.

of YDF1/P together with that of YDF1/Al [7]. In particular, one can see that the measured fluorescence lifetime of YDF1/P was reduced from 1.505 ms at 25ºC to 1.482 ms at 150ºC. The slight reduction of 1.53% in the fluorescence lifetime for the temperature difference (ΔT) of 125ºC indicates that there was a non-negligible change in the probability distribution of population among the Stark sublevels [6]. It is also noteworthy that the fluorescence lifetime of YDF1/P is substantially longer than that of YDF2/Al, which exhibited a lifetime decrease from 0.799 to 0.780 ms with increasing temperature from 10 to 100ºC. This led to a 2.38% reduction for ΔT = 90ºC, which is relatively larger than that of YDF1/P.

As described above, the lifetime reduction along with temperature variation resulted from the change of the population distribution among the Stark sublevels of Yb^{3+} ions, which would subsequently give rise to modifications to their absorption and emissions cross-sections. In general, the absorption cross-section can readily be calculated via the following relation [7, 23]:

$$\sigma_a(\lambda) = \frac{\alpha(\lambda)}{\Gamma(\lambda)N}, \tag{1}$$

where $\alpha(\lambda)$ is the absorption coefficient, $\Gamma(\lambda)$ the overlap factor between the doped area and the pump mode, N the total number density, i.e., the concentration, of Yb^{3+} ions, and λ the wavelength. The emission cross-section is also calculated via Füchtbauer-Ladenburg equation given by [7, 23, 24]

$$\sigma_e(\lambda) = \frac{\lambda^5}{8\pi c n^2 \tau_f} \frac{\mathrm{I}(\lambda)}{\int \lambda \mathrm{I}(\lambda) d\lambda} \tag{2}$$

where $I(\lambda)$ is the fluorescence intensity, and c, n, and τ_f denote the speed of light in vacuum, the refractive index of the medium, and the fluorescence lifetime, respectively. Thus, once the absorption coefficient and fluorescence

intensity are measured, one can readily determine the transition cross-sections.

Figure 2 represents all the calculated absorption and emission cross-sections of YDF1/P and YDF2/Al based on our experimental measurements for different temperature conditions. The inset figures represent the fiber facet images of YDF1/P and YDF2/Al, respectively. It is noteworthy that the noticeable peaks and valleys of the cross-section curves are due to the different combinatorial transitions among the Stark sublevels. In addition, the specific energies of the individual Stark sublevels are summarized in Table 1, which

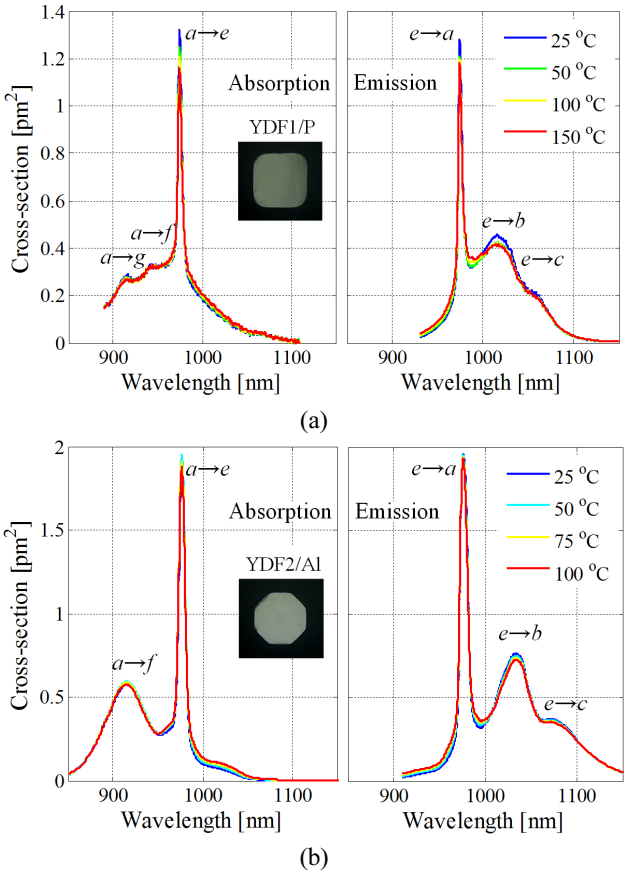

FIG. 2. Calculated absorption and emission cross-sections for (a) YDF1/P and (b) YDF2/Al for different temperature conditions. Inset: Fiber facet images of YDF1/P and YDF2/Al.

TABLE 1. The Stark energy-levels of YDF1/P and YDF2/Al

Energy Levels		YDF1/P [cm^{-1}]	YDF2/Al [cm^{-1}]
$^2F_{5/2}$	g	10915	11429
	f	10617	10922
	e	10262	10240
$^2F_{7/2}$	d	1087	1351
	c	810	937
	b	419	559
	a	0	0

were determined based on the emission and absorption spectra as well as their differential changes with temperature [14, 16]. Actually, the estimated energies both for YDF1/P and YDF2/Al result in similar trends with other YDFs of the previous results [14, 16] while there are a bit of differences due to the detailed compositional variations.

In Fig. 2(a), the peaks of the absorption cross-section of YDF1/P, which are observed from 915 nm to 950 nm, indicate the transitions of $a \rightarrow g$ and $a \rightarrow f$. The main peak observed at ~974 nm corresponds to the transition of $a \rightarrow e$. The transitions from "b" to upper sublevels represent the absorptions at longer wavelengths of 1030 nm to 1200 nm. Regarding the emission cross-section of YDF1/P, the main peak located at ~975 nm corresponds to the transition of $e \rightarrow a$. The transitions of $e \rightarrow b$, $e \rightarrow c$, and $e \rightarrow d$ correspond to the emissions peaks in the range of 1030 nm to 1200 nm. The valleys in the cross-sections also represent other combinatorial transitions among the sublevels. In particular, the valley near 960 nm represents the transition of $f \rightarrow b$ and $b \rightarrow f$.

The transition cross-sections of YDF2/Al are also shown in Fig. 2(b). While they presented similar trends to those of YDF1/P to some extent, a clear noticeable difference between YDF1/P and YDF2/Al is the behavior in the region around 940 nm. That is, the absorption cross-section of YDF1/P in that spectral band underwent significantly less thermal change compared to that of YDF2/Al. It should be noted that in that spectral region, YDF1/P and YDF2/Al form a plateau and a valley, respectively. As for the emission cross-sections, YDF1/P and YDF2/Al represent very similar behaviors, apart from the fact that the locations of the two main emission peaks in wavelengths above 1000 nm are substantially different: The two emission peaks of YDF1/P are located at much shorter wavelengths than those of YDF2/Al.

In addition, there are two significant, general trends in the changes of the transition cross-sections with temperature: One is that all the peaks related with the transitions to and from the lowest Stark sublevel, "a", decreases with temperature. The other is that the valleys related with the transitions between $f \rightarrow b$ and $b \rightarrow f$ become shallower with temperature. These are due mainly to the change in the population distribution of Yb^{3+} ions with temperature, which is primarily determined by the Boltzmann distribution law [22, 23]. In other words, if temperature increases, the populations in the upper sublevels of $^2F_{5/2}$ and $^2F_{7/2}$ will grow, and this will subsequently reduce the populations in the lower sublevels. Therefore, this boosted upward migration of the population among the Stark sublevels results in the changes in the transition cross-sections in such ways as observed in Fig. 2. To quantify these consequences more precisely, we plot in Fig. 3 the deviations ($\Delta\bar{\sigma}_a$ and $\Delta\bar{\sigma}_e$) of the transition cross-sections at 50 and 100°C against those at 25°C, which are normalized by their maximum values at 25°C in order to make a fair comparison between them.

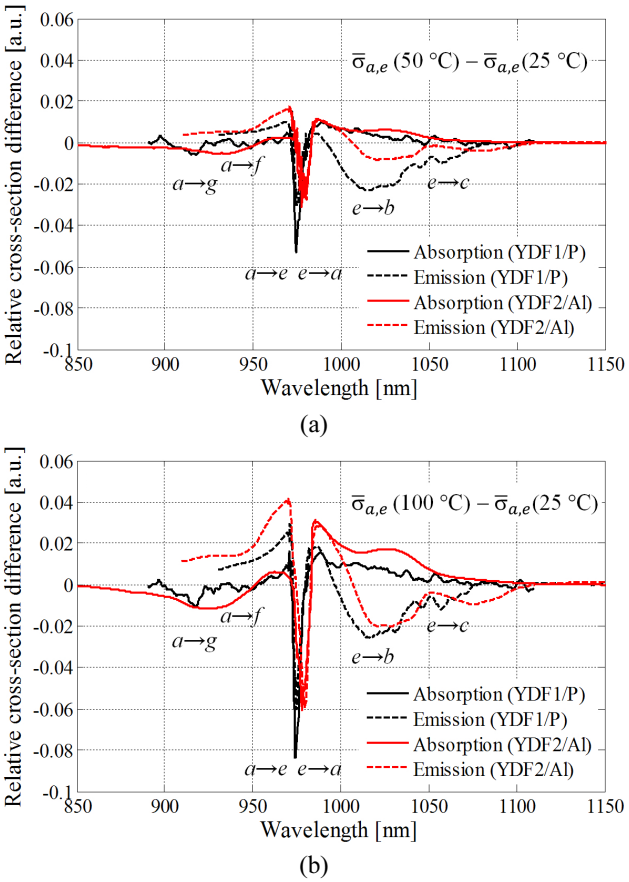

FIG. 3. Relative differences of the transition cross-sections at (a) 50 and (b) 100°C against those at 25°C. The transition cross-sections are normalized to their maximum values at 25°C.

As for $\Delta\bar{\sigma}_a$, there were clear indications of increasing quantities with temperature in the negative direction at around 920, 940, and 974 nm for YDF1/P, whereas at around 915 and 978 nm for YDF2/Al. These dips with negative quantities correspond to the transitions of $a \rightarrow g$, $a \rightarrow f$ and $a \rightarrow e$ for YDF1/P and those of $a \rightarrow f$ and $a \rightarrow e$ for YDF2/Al. In particular, for YDF1/P, the thermal deviation in the absorption cross-section is relatively flat and small in the spectral range of 920 nm to 950 nm, so that one can utilize this temperature insensitive spectral window for pumping, for example, pumping at 940 nm. However, this is not the case with YDF2/Al: Its absorption cross-section at 915 nm is significantly reduced with temperature. The peak absorptions at ~974 and ~975 nm for both cases exhibit relatively large variations with temperature. In addition, one can see that there were significant increases at the vicinity of ~975 nm and even longer wavelengths in both YDF1/P and YDF2/Al. These correspond to the transitions started from non-ground levels, such as $b \rightarrow f$ and $c \rightarrow g$, which must increase with temperature according to the Boltzmann distribution law [22, 23]. In particular, in the wavelength range longer than ~1020 nm, YDF1/P exhibits relatively smaller growth of the ground-state absorption in comparison with YDF2/Al.

As for $\Delta\bar{\sigma}_e$, the positive deviation is due mainly to the increase in the population in the upper Stark sublevels, such as, "f" and "g" levels whereas the negative deviation is due mainly to the decrease of the population in "e" level. In particular, one can find an intriguing point here that in the wavelength range longer than ~1020 nm, the absolute quantity of $\Delta\bar{\sigma}_e$ for YDF1/P becomes comparable or relatively smaller than that of YDF2/Al at the high temperature of 100°C whereas the former is significantly larger than the latter at the intermediate temperature of 50°C. This feature is more significantly seen in the wavelength range above ~1060 nm. In fact, such changes in the spectroscopic properties will lead to gain reductions with temperature because the signals at those wavelengths will undergo more absorption but will acquire less emission. It should be noted that the gain is primarily determined by the transition cross-sections as well as the inversion ratio, fluorescence lifetime, etc [22, 23]. Thus, one can expect that YDF1/P should perform better than YDF2/Al in high temperature conditions because the thermal variations of the former's transition cross-sections tend to become less in comparison with those of the latter. Hence, we further investigated the temperature-dependent gain characteristics of YDF1/P and YDF2/Al when they were used as gain fibers in a cladding-pumped amplifier configuration in the following. In particular, the amplifier configuration was chosen rather than a laser configuration because its gain is directly related with the spectroscopic properties of the gain fiber, including the transition cross-sections as well as the fluorescence lifetime [22, 23].

We newly set up a tunable seed fiber laser and a cladding-pumped amplifier based on YDF1/P. This was in an identical format with our previous arrangement for YDF2/Al [7] except for the pumping wavelength: YDF1/P was pumped at 940 nm whereas YDF2/Al was pumped at 915 nm. The gain fiber of YDF1/P used in the amplifier was 23-m long and was placed in the temperature-controlled oven. It should be noted that in a free-running laser configuration both fibers presented >70% of slope efficiencies with respect to absorbed pump power. Two different signal wavelengths of 1060 and 1080 nm were investigated for the temperature range of 25 to 100°C. The seed power to the amplifier was fixed to 150 mW during the whole measurements, and then, the amplifier was pumped to yield ~10-dB gain, i.e., the output power of ~1.5 W, which was exactly the same condition as our previous arrangement for YDF2/Al [7]. It is noteworthy that we restricted the maximum temperature to 100°C, which is well below the thermal damage threshold of the outer polymer material [12]. This was done in order to screen out any side effects due to the thermal degradation of the outer polymer material.

The gain characteristics of YDF1/P and YDF2/Al with temperature are shown in Fig. 4. It should be noted that

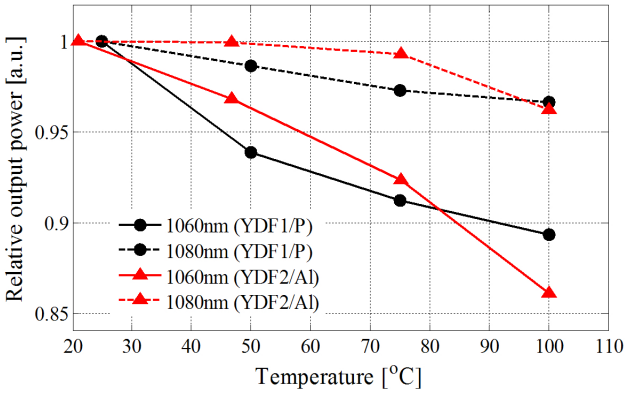

FIG. 4. Relative output powers of the cladding-pumped fiber amplifiers based on YDF1/P and YDF2/Al as a function of temperature. The output powers are normalized to their maximum values measured at ~25°C, which is ~1.5 W.

the output powers were normalized by their maximum values measured at ~25°C in order to make a fair comparison between them. One can see a similar overall trend of decreasing output power with temperature, which is basically determined by the thermal changes of the spectroscopic properties of the fibers as discussed above. Since Yb^{3+} ions behave much like a quasi-three-level system owing to the Stark split of $^2F_{7/2}$ which is not completely isolated from the ground state, they will suffer more ground-state absorptions if the signal wavelength becomes shorter. As temperature increases, the populations of "*b*" and "*c*" sublevels in $^2F_{7/2}$ manifold will gradually grow, which will lead to more ground-state absorptions for 1060 and 1080 nm and less stimulated emissions for them as well. However, the strengths of such changes will be greater for 1060 nm than for 1080 nm, as was verified in Fig. 3. This is why 1060 nm underwent more gain reduction than 1080 nm. While both YDF1/P and YDF2/Al presented similar gain reduction trends, they made a clear distinction when the temperature was elevated above ~80°C. That is, the gain reduction rate of YDF1/P was significantly reduced down as the temperature increased whereas that of YDF2/Al further rapidly grew. This behavior can actually be expected if the temperature-dependent spectroscopic properties of YDF1/P and YDF2/Al are compared, based on the results shown in Fig. 3. In addition, one can also notice in Fig. 3, the absorption of YDF2/Al at 915 nm (pump wavelength) was significantly reduced at the high temperature (100°C) condition, which would subsequently give rise to additional gain reduction due to the decrease in the absorbed pump power. On the contrary, the absorption change of YDF1/P at 940 nm (pump wavelength) was nearly negligible even at the high temperature condition.

III. CONCLUSION

We have measured and analyzed thermal characteristics of a P-based YDF (YDF1/P) in comparison with an Al-based YDF (YDF2/Al), including their spectroscopic properties and gain characteristics in the temperature range of 25 to 100ºC. While both fibers exhibited similar and comparable trends in their thermal characteristics, we could see several noticeable distinctions in terms of the fluorescence lifetime reduction rate, the spectral dependence of the transition cross-sections, and the gain reduction rate. In particular, the fluorescence lifetime of YDF1/P was much longer (~1.5 ms) than that of YDF2/Al (~0.8 ms), which implies that the lineshape broadening of the Yb^{3+} ions of the former must be smaller than that of the latter [22]. This can readily be seen in Fig. 3 or in Table 1. This, in fact, led to significantly less thermal lifetime reduction rate for YDF1/P (0.012%/ºC) than that for YDF2/Al (0.026%/ºC) [22]. Because of the narrower lineshape broadening of YDF1/P, the thermal changes of their transition cross-sections were more rapidly saturated in comparison with YDF2/Al. In addition, the absorption change of YDF1/P at 940 nm (pump wavelength) with temperature was nearly negligible. In result, YDF1/P exhibited better thermal resilience than YDF2/Al in terms of gain reduction, particularly, at higher temperatures over 80°C when they were used as gain fibers in a cladding-pumped amplifier configuration. In this light the shortcomings of the quasi-three-level nature of Yb^{3+} ions were better rectified in YDF1/P than in YDF2/Al in high-temperature conditions, which makes P-based YDFs attractive for stable, high-power operation, in particular, for operation at 1060 nm. A P-based YDF has also demonstrated sufficiently high thermal damage resilience for high-power operation: In Ref. 21, a record power extraction of 1.17 kW/m was successfully demonstrated, yielding the core temperature of well over 100°C [4,12]. Therefore, we conclude that P-based YDFs must be a good replacement of Al-based YDFs, considering their thermally stable characteristics as well as their substantially high PD resilience [15,19,21]. Our comprehensive experimental data and comparative analysis on YDF1/P and YDF2/Al could be further utilized in rigorous modeling on YDFs.

ACKNOWLEDGMENT

This work was supported in part by the Ministry of Knowledge Economy (Project No. 10040429).

REFERENCES

1. Y. Jeong, J. K. Sahu, D. N. Payne, and J. Nilsson, "Ytterbium-doped large-core fiber laser with 1.36 kW continuous-wave output power," Opt. Express **12**, 6088-6092 (2004).
2. D. J. Richardson, J. Nilsson, and W. A. Clarkson, "High power fiber lasers: current status and future perspectives," J. Opt. Soc. Am. B **27**, B63-B92 (2010).
3. J. Nilsson and D. N. Payne, "High-power fiber lasers," Science **332**, 921-922 (2011).

4. Y. Wang, C. Q. Xu, and H. Po, "Thermal effects in kilowatt fiber lasers," IEEE Photon. Technol. Lett. **16**, 63-65 (2004).
5. T. C. Newell, P. Peterson, A. Gavrielides, and M. P. Sharma, "Temperature effects on the emission properties of Yb-doped optical fibers," Opt. Commun. **273**, 256-259 (2007).
6. X. Peng and L. Dong, "Temperature dependence of ytterbium-doped fiber amplifiers," J. Opt. Soc. Am. B **25**, 126-130 (2008).
7. L. A. Vazquez-Zuniga, S. Chung, and Y. Jeong, "Thermal characteristics of an ytterbium-doped fiber amplifier operating at 1060 and 1080 nm," Jpn. J. Appl. Phys. **49**, 022502-1~022502-5 (2010).
8. M. J. Söderlund, J. Ponsoda, J. P. Koplow, and S. Honkanen, "Heat-induced darkening and spectral broadening in photo-darkened ytterbium-doped fiber under thermal cycling," Opt. Express **17**, 9940-9946 (2009).
9. S. Yoo, A. J. Boyland, R. J. Standish, and J. K. Sahu, "Measurement of photodarkening in Yb-doped aluminosilicate fibres at elevated temperature," Electron. Lett. **46**, 233-234 (2010).
10. M. Leich, S. Jetschke, S. Unger, and J. Kirchhof, "Temperature influence on the photodarkening kinetics in Yb-doped silica fibers," J. Opt. Soc. Am. B **28**, 65-68 (2011).
11. J. Ponsoda, C. G. Ye, J. P. Koplow, M. J. Söderlund, J. J. Koponen, and S. Honkanen. "Analysis of temperature dependence of photodarkening in ytterbium-doped fibers," Opt. Eng. **50**, 111610 (2011).
12. Y. Jeong, S. Baek, P. Dupriez, J.-N. Maran, J. K. Sahu, J. Nilsson, and B. Lee, "Thermal characteristics of an end-pumped high-power ytterbium-sensitized erbium-doped fiber laser under natural convection," Opt. Express **16**, 19865-19871 (2008).
13. Y. Jeong, J. Nilsson, J. K. Sahu, D. N. Payne, R. Horley, L. M. B. Hickey, and P. W. Turner, "Erbium:ytterbium codoped large-core fiber laser with 297-W continuous-wave output power," IEEE J. Select. Topics Quantum Electron. **13**, 573-579 (2007).
14. M. A. Melkumov, I. A. Bufetov, K. S. Kravtsov, A. V. Shubin, and E. M. Dianov, "Lasing parameters of ytterbium-doped fibres doped with P_2O_5 and Al_2O_3," Quantum Electron. **34**, 843-848 (2004).
15. M. Engholm and L. Norin, "Preventing photodarkening in ytterbium-doped high power fiber lasers; correlation to the UV-transparency of the core glass," Opt. Express **16**, 1260-1268 (2008).
16. S. Suzuki, H. A. McKay, X. Peng, L. Fu, and L. Dong, "Highly ytterbium-doped silica fibers with low photo-darkening," Opt. Express **17**, 9924-9932 (2009).
17. J. J. Koponen, M. J. Söderlund, H. J. Hoffmann, and S. K. T. Tammela, "Measuring photodarkening from singlemode ytterbium doped silica fibers," Opt. Express **14**, 11539-11544 (2006).
18. J. Jasapara, M. Andrejco, D. DiGiovanni, and R. Windeler, "Effect of heat and H_2 gas on the photo-darkening of Yb^{+3} fibers," in *Proc. CLEO/QELS* (Long Beach, USA, May 2006), paper CTuQ5.
19. V. Shubin, M. V. Yashkov, M. A. Melkumov, S. A. Smirnov, I. A. Bufetov, and E. M. Dianov, in *Proc. CLEO/IQEC* (Munich, Germany, Jun. 2007), paper CJ3_1.
20. Y. W. Lee, S. Sinha, M. J. F. Digonnet, R. L. Byer, and S. Jiang, "Measurement of high photodarkening resistance in heavily Yb^{3+}-doped phosphate fibres," Electron. Lett. **44**, 14-16 (2008).
21. A. Codemard, A. Shirakawa, J. K. Sahu, S. Yoo, Y. Jeong, and J. Nilsson, "Thermal resilience of polymer-coated double-clad fiber," in *Proc. CLEO/EQEC* (Munich, Germany, Jun. 2009), paper CJ_P5.
22. W. Koechner, *Solid-state Laser Engineering* (Springer, London, UK, 1999).
23. E. Desurvire, *Erbium-doped Fiber Amplifiers* (Wiley, New York, USA, 1994).
24. X. L. Zou and H. Toratani, "Evaluation of spectroscopic properties of Yb^{3+}-doped glasses," Phys. Rev. B **52**, 15889-15897 (1995).